RECENT ADVANCES IN INTEGRATED MULTIDISCIPLINARY OPTIMIZATION OF ROTORCRAFT

Howard M. Adelman*, Joanne L. Walsh** and Jocelyn I. Pritchard†
NASA Langley Research Center
Hampton, Virginia

Abstract

This paper describes a joint activity involving NASA and Army researchers at the NASA Langley Research Center to develop optimization procedures to improve the rotor blade design process by integrating appropriate disciplines and accounting for all of the important interactions among the disciplines. The disciplines involved include rotor aerodynamics, rotor dynamics, rotor structures, airframe dynamics, and acoustics. The work is focused on combining these five key disciplines in an optimization procedure capable of designing a rotor system to satisfy multidisciplinary design requirements. Fundamental to the plan is a three-phased approach. In phase 1, the disciplines of blade dynamics, blade aerodynamics, and blade structure are closely coupled while acoustics and airframe dynamics are decoupled and are accounted for as effective constraints on the design for the first three disciplines. In phase 2, acoustics is integrated with the first three disciplines. Finally, in phase 3, airframe dynamics is integrated with the other four disciplines. Representative results from work performed to date are described. These include optimal placement of tuning masses for reduction of blade vibratory shear forces, integrated aerodynamic/dynamic optimization, and integrated aerodynamic/dynamic/structural optimization. Examples of validating the procedures are described.

* Deputy Head, Interdisciplinary Research Office, Associate Fellow AIAA, Member AHS, ASME
** Research Engineer, Interdisciplinary Research Office, Member AIAA, AHS
† Research Engineer, AVSCOM Aerostructures Directorate, Member AHS

Introduction

An emerging trend in the analytical design of aircraft is the integration of all appropriate disciplines in the design process.[1-2] This means not only including limitations on the design from the various disciplines, but also defining and accounting for interactions so that the disciplines influence design decisions simultaneously rather than sequentially. In rotorcraft design, the appropriate disciplines include aerodynamics, dynamics, structures and acoustics. This paper describes an activity for developing the logic elements for helicopter rotor design optimization which includes the above disciplines in an integrated manner.

Rotorcraft design is an ideal application for integrated multidisciplinary optimization. In current design practice however, the process has generally been sequential, (i.e. single-discipline oriented)[3-6] rather than integrated. In early 1985, several occurrences led the NASA Langley Research Center to address the multidisciplinary design problem. The Interdisciplinary Research Office within the NASA Langley Structures Directorate was charged with the development of integrated multidisciplinary optimization methods. Nearly concurrently, the Army Aerostructures Directorate at Langley established the goal of improving rotorcraft design methodology by "discipline integration." Close cooperation between the NASA and Army organizations led to plans for a comprehensive research program for an integrated analytical design capability. As a result of the common goals in rotorcraft design, a group of NASA/Army researchers (referred to herein as the Langley Team) initiated the approach described in this paper.

The focus of the NASA/Army research is to develop strategies, logic, and formulations for integrated multidisciplinary design optimization with a view toward their application in the rotorcraft community. Toward this end, the Langley Team produced a comprehensive plan[7] which was sent to each of the principal helicopter companies in the United States to obtain their critique. Subsequently, the Langley Team completed a tour of the companies

to review the results of the critiques. An updated plan was produced which was more representative of industry design philosophies and guides the ongoing research. The purpose of this article is to describe the plan and to summarize the most recent results and progress in the work. Specifically, the paper contains a summary of the plan, the sequence of the development, and some recent results. These results include optimal placement of tuning masses for reduction of blade vibratory shear forces, integrated aerodynamic/dynamic optimization, and formulation for integrated aerodynamic/dynamic/structural optimization.

General Approach and Scope

Development Strategy

A three-phased approach for the activity is illustrated in figure 1. In phase 1 the rotor blade aerodynamics, dynamics and structural analyses are

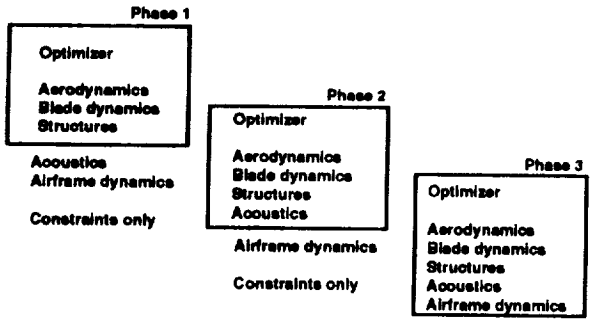

Fig. 1 Three-phase development strategy for rotorcraft optimization

coupled and driven by the optimizer. The optimization of the blade aerodynamic geometry, blade stiffness and mass distributions and the detailed internal structure is performed. The design requirements influenced by the acoustics and airframe dynamics are accounted for indirectly by constraints on the blade design. In phase 2 the acoustic analysis is fully integrated with the blade aerodynamics, dynamics, and structural analysis. Constraints will include limits on sound pressure levels and directivity. The design produced in phase 2 will satisfy acoustics goals. Airframe dynamics in phase 2, as in phase 1, is accounted for by effective constraints on the blade dynamics, aerodynamics and structural behavior. Finally, in phase 3, airframe dynamics is integrated and the result is a fully integrated optimization strategy.

Sequence of Tasks for Phase 1

Figure 2 depicts the general sequence of single and dual discipline optimization tasks that lead to a fully-integrated rotor blade aerodynamic/dynamic/structural optimization procedure. The dynamic optimization bubble in the figure represents the work from references 5, 6, and 8-11. The aerodynamic performance optimization bubble is based on the work described in reference 12. The left-center bubble represents the integration of an aerodynamic loads analysis with dynamics; a procedure wherein the airloads can be adjusted by changes in the design variables to reduce dynamic response. This work is described in reference 13. The arrows leading from these three bubbles indicate that a merger of these three produced a fully integrated aerodynamic/dynamic procedure described in reference 14. The structural optimization bubble indicates that some work in rotor structural optimization was being initiated simultaneously with the integrated work and is discussed in reference 15. The strategy for integration of the structural optimization with the dynamics and aerodynamics represented by the bubble on the far right is a multilevel formulation based on the theory described in references 16 and 17. In the present formulation, the planform shape, pretwist, stiffnesses and mass distributions of the blade are determined in the upper level and the detailed sizing of the blade spar takes place in the lower level.

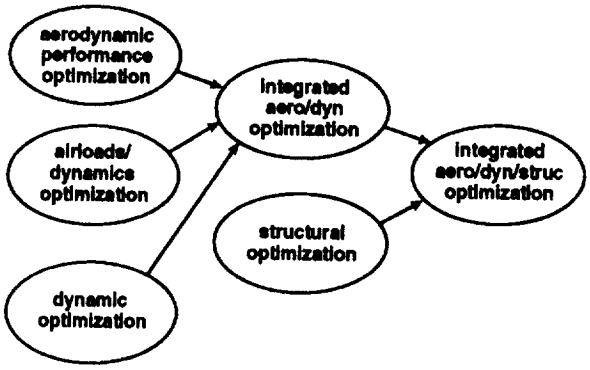

Fig. 2 Sequence of optimization elements for phase I

Status/Results

The development of the strategies for the elements in figure 2 is nearly complete. Validated demonstrations of optimum placement of tuning masses for vibration reduction, integrated aerodynamic/dynamic optimization, and the strategy for integrated aerodynamic/dynamic/structural optimization are highlighted in this section of the paper.

Optimum Locations of Vibration Tuning Masses

The objective of this work was to develop and validate a dynamic optimization procedure that systematically determines the best values and locations for tuning masses for reducing vibratory vertical hub shear. Optimal placement of the mass tailors the mode shapes and airloads thus reducing generalized force and response of the blade. The method entails formulating an optimization procedure that employs the tuning masses and their locations as design variables to minimize vertical hub shear with the smallest possible mass penalty. Equation (1) defines the objective function, f, which is a combination of vertical hub shear and added mass where K is the number of shear harmonics to be included in the objective function, M_j is the jth tuning mass, and S_{ref} is a reference value of vertical hub shear.

$$f = \left(1 + \frac{1}{S_{ref}} \sum_{k=1}^{K} \beta_k\right) \sum_{j=1}^{J} M_j \qquad (1)$$

The additional design variables, β_k, which appear in the objective function (equation 1) and the constraints shown below in equation (2) are "pseudo upper limits" on the calculated shear harmonic amplitudes, S_k,

$$S_k / \beta_k - 1 \le 0 \qquad k = 1,2,\ldots,K \qquad (2)$$

These constraints express the requirement that S_k be less than the value of β_k. Consequently, the optimizer will tend to increase the values of β_k to satisfy the constraints but at the same time will attempt to decrease the values of β_k to minimize the objective function. This results in a compromise on the values of β_k which forces a reduction in the values of S_k thus reducing the hub shear harmonics while incurring the smallest possible mass penalty. Additional constraints include upper and lower bounds on the first two flapwise frequencies of the blade to avoid resonance as shown in equation (3)

$$\left.\begin{aligned} \bar{\omega}_i / \omega_{ui} - 1 \le 0 \\ 1 - \bar{\omega}_i / \omega_{li} \le 0 \end{aligned}\right\} \qquad i = 1,2,\ldots,I \qquad (3)$$

where $\bar{\omega}_i = \omega_i / \Omega$, ω_i is the ith natural frequency, ω_{ui} and ω_{li} are the upper and lower bounds on the frequency, respectively, Ω is the blade rotational speed, I is the number of constrained frequencies.

As described in detail in reference 10, the implementation of the approach was to combine the optimizer CONMIN[18] with CAMRAD/JA[19]. The latter code was used to calculate mode shapes, frequencies, airloads and hub shears. The use of CAMRAD/JA enables the variation in the airloads due to changes in the design variables to be taken into account.

The bar chart in figure 3 compares the results of applying the optimization procedure to place three masses and six masses on a one-sixth, Mach-scaled

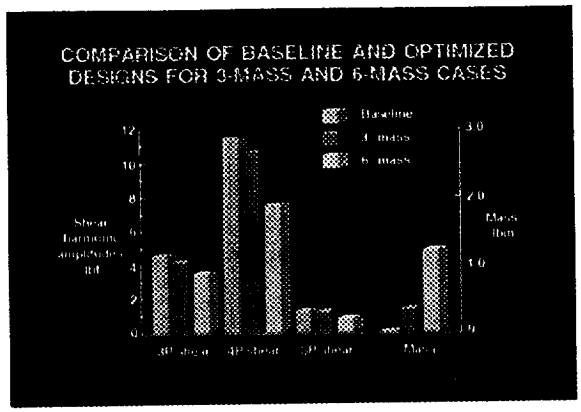

Fig. 3 Results for optimal placement and sizing of three and six masses

model of the growth version of the U. S. Army's UH-60A helicopter rotor blade. The axis on the left measures the shear harmonic amplitudes and the axis on the right measures the amount of tuning mass that was added. The groups of columns from left to right represent the third, fourth, and fifth harmonics of shear and the mass, respectively. The columns within each group from left to right represent the values of the baseline which has no added mass, the three-mass case and the six-mass case, respectively. Using three masses, the procedure was able to reduce the shear by about eight percent for the third and fourth harmonics and four percent for the fifth with a ten percent increase in total blade weight. Using six masses, the third harmonic was reduced by 24 percent from the nominal, the fourth harmonic was reduced 34 percent, and the fifth harmonic 32 percent. The amount of mass that was needed to achieve these reductions was approximately a 30 percent increase in the total blade weight which would probably disqualify this blade in practice. However, this result shows that the method trades shear reduction for mass and it confirms the hypothesis that large reductions in vibratory shear require a large mass penalty.

As described in reference 10, the procedure has also been applied to a blade test article (shown in figure 4) that has the capability for adding tuning masses

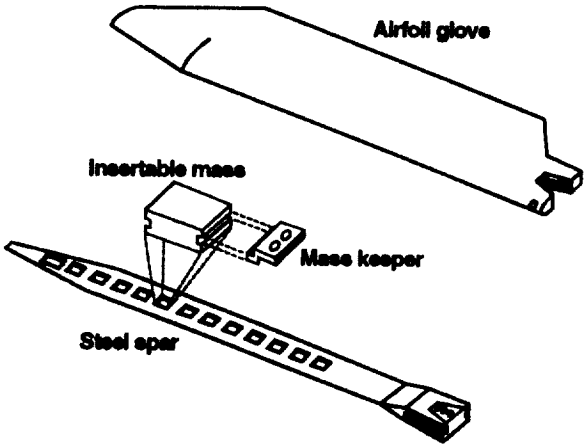

Fig. 4 Test article for experimental validation of mass placement method

along the blade span. The test article, designed to study passive means for minimizing fixed-system loads, was tested in the Langley Transonic Dynamics Tunnel. The test data included 4/rev hub shear as a function of the location of a single tuning mass of 0.27 lbm for several flight conditions. The graph in figure 5 shows the comparison between the optimization results and the test data for three advance ratios (0.25, 0.30, and 0.35). The test data is shown as a band since the data was available only at ten per-

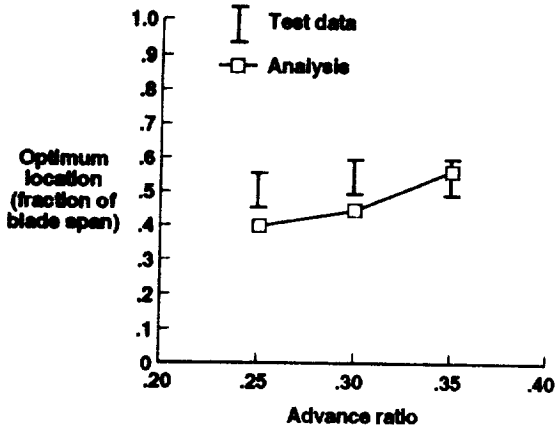

Fig. 5 Comparison of optimum locations of single mass with test data

cent increments along the span. For the 0.35 advance ratio case, the optimization procedure predicted an optimum location that was within the range of the test data. For the other two cases (0.25 and 0.30) the predictions were respectively eleven percent and twelve percent below the range. This is fairly good agreement considering the difficulty of predicting fixed-systems loads with existing analysis codes.

Integrated Aerodynamic/dynamic Optimization (AD)

A fully integrated aerodynamic/dynamic optimization procedure[14] which combines performance and dynamics analyses for hover, forward flight, and maneuver with a general purpose optimizer has been developed. The maneuver flight condition simulates a sustained pull-up maneuver in terms of a load factor on the forward flight lift requirement.

Objective Function - The procedure minimizes an objective function which is a composite measure of performance and dynamics. Specifically, the objective function is a linear combination of power required (for hover, forward flight, and maneuver) and vibratory hub shear

$$F = k_1 \frac{HP_h}{HP_{h_{ref}}} + k_2 \frac{HP_{ff}}{HP_{ff_{ref}}} + k_3 \frac{HP_m}{HP_{m_{ref}}} + k_4 \frac{S_{N_{ff}}}{S_{N_{ref}}} \qquad (4)$$

where HP_h, HP_{ff}, and HP_m are the powers required in hover, forward flight, and maneuver, respectively. $S_{N_{ff}}$ is the N per rev nonrotating vertical hub shear in forward flight and N is the number of blades. The terms k_1, k_2, k_3, and k_4 are weighting factors. $HP_{h_{ref}}$, $HP_{ff_{ref}}$, $HP_{m_{ref}}$, and $S_{N_{ref}}$ are reference values used to normalize and nondimensionalize the objective function components.

Design Variables - The design variables are shown in figure 6 and consist of aerodynamic quantities describing the blade planform and pretwist and of dynamic quantities describing the blade structural properties. The four aerodynamic design variables are

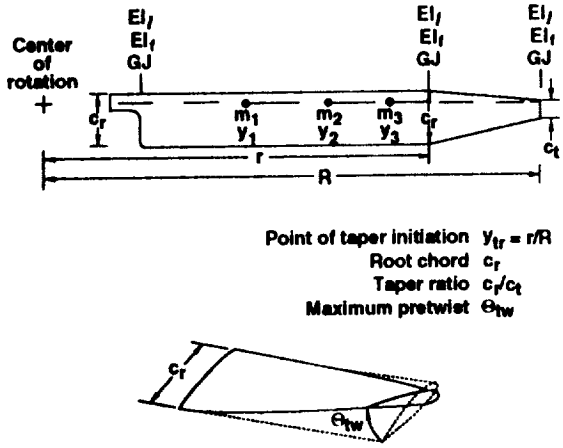

Fig. 6 Design model for integrated aerodynamic/dynamic optimization

the point of taper initiation y_{tr}, root chord c_r, taper ratio c_r/c_t, and maximum pretwist Θ_{tw}. The blade is rectangular to y_{tr} and then tapers linearly to the tip. The pretwist (blade structural and aerodynamic twist are assumed to be the same) varies linearly from the center of rotation to the tip. Nine dynamic design variables include the blade stiffnesses in the lagwise (inplane) and flapwise (vertical) directions (denoted by EI_l and EI_f) and torsional stiffnesses (denoted by GJ) at the blade root, point of taper initiation, and blade tip. The stiffnesses are assumed to vary linearly between these three points. The remaining six dynamic design variables are three tuning masses (denoted by m_1, m_2, and m_3) and their distances from the center of rotation (denoted by y_1, y_2, and y_3). The total blade mass consists of the structural mass (which remains constant) plus the sum of the tuning masses.

Constraints - The constraints are grouped into performance constraints and dynamic constraints. The performance constraints are imposed for all three flight conditions. The dynamic constraints are imposed only in forward flight and maneuver. The blade is designed for a constant lift in forward flight and a constant lift in maneuver.

The performance constraints are on power required, stall, trim, and blade tip chord. The limit on power is that the power required in hover, forward flight, and maneuver be less than the power available. The requirements that the airfoil sections not stall and that the drag divergence Mach number are avoided are expressed as upper limit constraints on the airfoil section drag coefficients as functions of the angle of attack and Mach number. These constraints are evaluated at every 15 degrees around the azimuth in forward flight and maneuver. An isolated rotor analysis is used which trims the rotor to constant lift and drag and zero flapping angle relative to the shaft using collective, lateral cyclic and longitudinal cyclic pitch. Trimming to a constant lift ensures that the rotor retains the specified lift capability even if solidity decreases. The trim constraint is implemented in forward flight and maneuver. The final performance requirement is a lower limit on the blade tip chord.

The dynamic constraints are "windows" on frequencies, total blade weight, and autorotational inertia. The constraint on frequency (either a bending or a torsional frequency) avoids integer multiples of the rotor speed Ω. The constraint on blade mass sets the maximum value (the total blade mass is the sum of the constant structural mass and the tuning masses) and the constraint on autorotational inertia requires safe autorotation in case of engine failure.

Rotor Analyses - The analyses used in this work are the Langley-developed hover analysis program HOVT (a strip theory momentum analysis based on reference 20) and the comprehensive helicopter analysis program CAMRAD/JA for forward flight and maneuver. HOVT is used to predict power required in hover using nonuniform inflow (no wake is included). CAMRAD/JA is used to calculate rotor performance, loads, and frequencies. In this work the CAMRAD/JA analyses are performed with uniform inflow with empirical inflow correction factors. Both HOVT and CAMRAD/JA use tables of experimental two-dimensional airfoil data.

Optimization Methods - The codes used for optimization are the general purpose optimization program CONMIN and an approximate analysis used to reduce the number of HOVT and CAMRAD/JA analyses during the iteration process. CONMIN is a general purpose optimization program which uses the method of usable-feasible directions for constrained function minimization. The approximate analysis is used to extrapolate the objective function and constraints with linear Taylor Series expansions using derivatives of the objective function and constraints with respect to the design variables. The assumption of linearity is valid over a suitably small change in the design variable values and will not introduce a large error into the analysis provided the changes are small. Errors which may be introduced by use of the approximate analysis are controlled by imposing "move limits" on each design variable during the iteration process. A move limit which is specified as a fractional change of each design variable value is imposed as an upper and lower design variable bound.

Implementation of Optimization Procedure- The optimization procedure (figure 7) consists of an outer loop denoted by "Cycle" and an inner loop denoted by "Iteration". First, preassigned parameters

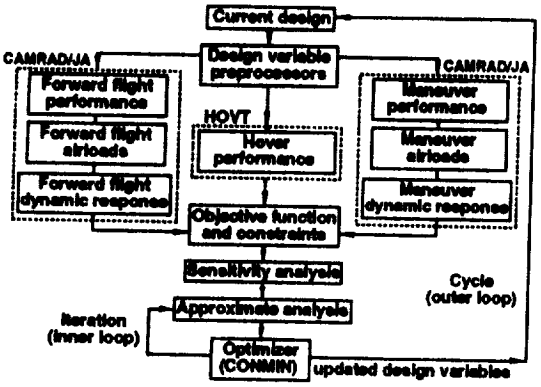

Fig. 7 Flowchart for integrated aerodynamic-dynamic optimization

such as the blade radius, airfoil distribution, and number of blades are set. An optimization cycle is initiated. The aerodynamic and structural properties such as twist and chord distributions, radial station locations, solidity, blade weight, and autorotational inertia are calculated using the current design variable values in the box labelled "Design variable preprocessors". The HOVT analysis is then performed to obtain the power required in hover. Two CAMRAD/JA analyses (forward flight and maneuver) are then performed to obtain the power required, trim information, coefficients of drag for the stall constraints, natural frequencies, and hub shears. This information is then used to formulate the objective function and constraints. Since CONMIN and the approximate analysis need derivatives of the objective function and constraints, a sensitivity analysis is performed to obtain finite difference derivatives of the objective function and constraints with respect to the design variables. These derivatives are obtained by perturbing each design variable one at a time and going through the design variable preprocessor, HOVT, and CAMRAD/JA analyses. The inner loop consists of CONMIN and the approximate analysis. New values for the design variables are obtained and the outer loop is re-entered. Convergence is obtained if the objective functions from three consecutive cycles are the same within a tolerance of 0.5×10^{-5}.

Validation by Comparison with Conventionally-designed Blade - The procedure was tested from an arbitrary starting point to determine how well it could reproduce the design of an existing wind tunnel model of a growth utility rotor blade which was designed previously by conventional methods (not using formal optimization techniques). This existing blade will be referred to as the actual blade. This blade has a rectangular planform to 0.80R (80 percent radius) and then tapers to the tip with a 3-to-1 taper ratio. The blade has a radius of 56.22 inches and a root chord of 5.40 inches.

The flight conditions are (1) a constant lift of scaled 1-g (331 pounds), propulsive force of 32 pounds, and an advance ratio of 0.35 for the forward flight condition and (2) a constant lift of 401 pounds, a propulsive force of 23 pounds, and an advance ratio of 0.3 for the maneuver flight condition. The maneuver flight condition has a load factor of 1.22. Since f_1 corresponds to a rigid body mode and f_2 is the 1 per rev, the first two frequencies are not constrained. Constraints are placed on the first four bending frequencies (f_3 through f_6) and the first two torsional frequencies (t_1 representing the rigid body torsional mode due to the control system stiffness and t_2 representing the first elastic torsional mode). The analysis of the blade calculates a total weight of 3.05 lbs and an autorotational inertia value of 3411 lbm-in^2. The blade is to be designed so that the weight is not increased by more than 15 percent and the autorotational inertia is increased by at least 1 percent from that of the actual blade. The values for minimum tip chord, power available, and maximum allowable drag coefficient are 1 in, 20 hp, and 0.1, respectively. A frequency window of ± 0.1 per rev is used for the frequency constraints.

The initial trial blade design (the starting point for the optimization) is a blade which has a rectangular planform with a maximum pretwist of -9.0 degrees and blade root chord of 5.40 in. This blade has the same root chord, mass distribution, and stiffness distributions at the root, 0.8R (point of taper initiation of the actual blade), and the tip as the actual blade. The stiffnesses are assumed to vary linearly between these points. The nonstructural mass distribution depends only on the tuning masses and their locations. Note that the initial blade does not satisfy the minimum autorotational inertia requirement.

Since a four-bladed rotor is used as the test problem, the 4 per rev nonrotating hub shear is used for $S_{N_{ff}}$ in the objective function given by equation 4. The normalizing factors $HP_{h_{ref}}$, $HP_{ff_{ref}}$, and $HP_{m_{ref}}$ are each chosen to be 15 hp and $S_{N_{ref}}$ is chosen to be 2 lbf (based on analysis of the initial blade). The actual blade was originally designed for performance. Therefore, the objective function is chosen to be one dominated by performance with little emphasis on

dynamics. Of the three flight conditions, it is assumed that it is most important to reduce the power required in hover - therefore, this term will have twice the weight as the other two horsepower terms. Several values were tried for the weighting factor on the hub shear term. It was found that to obtain the proper balance between performance and dynamics, k_4 has to be about three orders of magnitude smaller than k_1. Thus, for this case, the weighting factors are chosen to be k_1 =15.0, k_2=k_3=7.5, and k_4 = 0.025.

Figure 8 includes the shape and response for the initial trial, final, and actual blades. The figure shows comparison of performance and dynamics measures (horsepower for hover, forward flight, and maneuver and the 4 per rev forward flight vertical hub shear). The final design has the same pretwist as the actual blade. Both planforms are similar with the final design having less solidity than the actual blade. Specifically, the root chord was 4.4 in, the taper ratio was 1.8, the point of taper initiation was 0.68, and the maximum pretwist was -16 degrees. For the actual blade these values were 5.4 in, 3.0, 0.80, and -16 degrees, respectively. The difference in planforms is primarily due to the choice of flight conditions. The actual blade was designed by use of parametric studies for slightly different flight conditions and design requirements.

	Initial trial design	Final design	Actual blade
Hover hp	15.35	14.41	14.84
Forward flight hp	13.52	12.54	13.13
Maneuver hp	12.26	11.78	11.83
4 per rev hub shear lbf	2.19	1.17	1.52

Fig. 8 Comparison of optimization-based design with actual blade

Validation By Use of Test Article

The AD procedure has been used to design a test article which will be used to validate the procedure through wind-tunnel testing. Along with a baseline blade, the validation blade will be tested for aerodynamic and dynamic performance in the Transonic Dynamics Tunnel (TDT) at Langley. The baseline blade was previously designed by the U.S. Army Aerostructures Directorate at the Langley Research Center and was made available to the Langley Team for use in the current work. The purpose of the tests will be twofold: to verify that the optimization procedure can produce a blade that will improve the aerodynamic and dynamic performance relative to a baseline design; and to verify the behavior and trends predicted by the analytical procedures.

The validation blade was designed for a five-bladed rotor for the following conditions: in hover, a constant 1.0 g scaled lift of 301 lb; in vertical rate of climb of 1000 ft/min; in forward flight, a constant 1.0 g lift of 301 lb and a constant propulsive force of 28 lbs at an advance ratio of 0.326; a maneuver simulated by a load factor of 2.0 g (602 lb) at an advance ratio of 0.233 with a propulsive force of 9.0 lbs. The objective function is that shown in equation (4) with the following weighting factors: k_1 = 1.0 k_2 = 1.0 k_3 = 0.5 k_4 = 1.0. The optimization procedure was carried out with the initial blade design being the baseline blade which has a rectangular planform and pretwist of -8.0 degrees. The CAMRAD/JA analysis employed in the analyses used a wake model with rigid geometry with vertical convection by the mean inflow.

	Baseline	Optimized
twist (deg)	-8.00	-14.30
taper init	—	0.79
taper ratio	1.00	1.60
root chord (in)	4.45	4.63
hover hp	14.42	13.50
ff hp	12.93	12.50
man hp	25.39	24.30
e_5 (lbf)	1.07	1.05

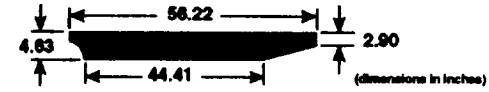

0.023	22.9
0.035	29.4
0.400	29.5

Fig. 9 Validation test article

Figure 9 shows the results of the optimization. The analytical predictions in the upper Table show a predicted improvement in hover power, forward flight power and maneuver power of six percent, three percent, and four percent, respectively. The improvement in vibratory load level is predicted to be minimal. The validation test article is presently in the fabrication stage and testing is expected to be initiated during calendar year 1993.

Integrated Aerodynamic-Dynamic-Structural Optimization (ADS)

Multilevel Optimization Strategy

The ADS optimization strategy is based on the method of multilevel decomposition described in references 16 and 17. In this case there are two levels.

In the upper level (figure 10) the goal is to optimize a combination of aerodynamic and dynamic performance while satisfying constraints on the aerodynamic, dynamic and global structural behavior (i.e., average strain). The upper level is essentially the same as the AD

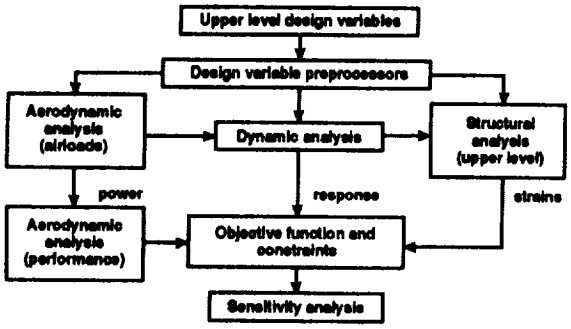

Fig. 10 Upper level of integrated aerodynamic-dynamic-structural optimization

procedure with the addition of strain constraints, design variables representing section masses M (including structural and non-structural mass but excluding tuning masses), extensional stiffness variables EA at several spanwise locations, and coordination constraints which link the upper and lower levels.

In the lower level (figure 11), the sizing of the internal blade structure takes place. The purpose of the lower level optimization is to assure that a structure can be sized to provide the required stiffnesses and section masses needed at the upper level and also to assure the structural integrity of the blade. The lower level optimization is performed in parallel for several spanwise cross sections. As indicated in figure 11, the EI*, GJ*, EA*, and M*

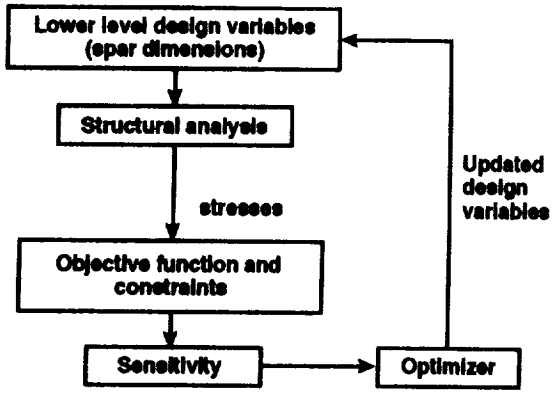

Fig. 11 Lower level of integrated aerodynamic-dynamic-structural optimization

design variables from the upper level are passed to the lower level. The lower level objective function for each section is a measure of how close the EI's, GJ and M are to those required at the upper level. Constraints are enforced at each section to assure that the lower level produces an EA which is at least as large as that required in the upper level. Constraints are also enforced on the axial and shear stresses in the blade.The design variables are the detailed dimensions of the blade cross sections.

Example of ADS Procedure

An example of the ADS optimization procedure is described in this section of the paper. For illustrative purposes and simplicity, it is assumed that the blade is constructed from an isotropic material. Although no numerical results from this formulation are included in the paper, this example is the basis for numerical calculations which are in progress for demonstrating the methodology.

Upper Level Objective Function - The objective function is a combination of rotor horsepower and transmitted vibratory loads at several flight conditions

$$F = k_1 \frac{HP_h}{HP_{h_{ref}}} + k_2 \frac{HP_{ff}}{HP_{ff_{ref}}} + k_3 \frac{HP_m}{HP_{m_{ref}}} + k_4 \frac{S_{N_{ff}}}{S_{N_{ref}}} \qquad (5)$$

where F is the objective function, k_i are weighting factors, HP_i are horsepowers for three flight conditions listed below, $S_{N_{ff}}$ is the N/rev vertical hub shear in forward flight, and HP_{ref} and $S_{N_{ref}}$ are reference values of horsepower and load respectively. The set of flight conditions is:

Flight condition	Description	Advance ratio	Load factor
1	hover	0	1.0
2	forward flight	0.35	1.0
3	maneuver	0.30	1.22

Upper Level Design Variables - The design model is shown in figure 12. The design variables

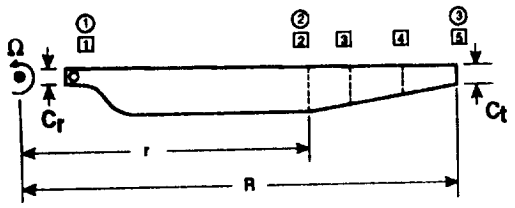

○ Location where upper level design variable defined
□ Location where lower level optimization performed

(a) Upper level

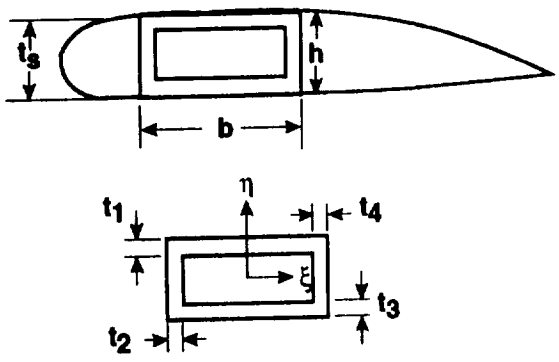

(b) Lower level

Fig. 12 Design model for integrated aerodynamic/dynamic/structural optimization

(depicted on the blade schematic) include EI_f, EI_l, GJ, EA, and M (at the three spanwise locations indicated by the circled numbers), three tuning masses and locations, c_r, $\lambda=c_r/c_t$, y_{tr}, and Θ_{tw}.

Upper Level Constraints - The upper level constraints are the same as those in the AD procedure with the addition of strain constraints and "coordination" constraints which assure proper linkage and consistency between the upper and lower levels. These constraints are imposed at several spanwise locations (currently five) denoted in figure 12(a) by the numbered boxes. The locations are the blade root, point of taper initiation, tip, at the two locations where the airfoils change (r/R = 0.85 and r/R = 0.95). The constraints imposed on the average axial strains ε_x are as follows:

$$\varepsilon_x / \varepsilon_a - 1 \le 0 \tag{6}$$

where ε_a is the allowable strain and

$$\varepsilon_x = N/EA \tag{7}$$

In equation (7), N is the centrifugal force, and EA is the extensional stiffness. The "coordination" constraints will be defined in detail after the lower level optimization is described.

Lower Level Objective Function - As indicated previously, a lower level optimization is performed for each of five cross sections. In each section, the objective function is as follows.

$$F = \left(\left(EI_f - EI_f^*\right)/EI_f^*\right)^2 + \left(\left(EI_l - EI_l^*\right)/EI_l^*\right)^2 + \left(\left(GJ - GJ^*\right)/GJ^*\right)^2 + \left(\left(M - \delta M^*\right)/\delta M^*\right)^2 \tag{8}$$

In equation 8 a starred quantity ( )* denotes a design variable from the upper level and δ represents a fraction of the upper level mass M*. The box beam designed in the lower level represents structural mass, therefore only the structural mass portion of M^* is matched in the lower level. Typically, δ is chosen to be 0.6 which would require the structural mass of the box in the lower level to be 60 percent of the total upper level mass. The cross sectional properties I_l, I_f, and J are computed according to engineering theory of thin-walled beams[21] from the dimensions of the section (b,h,t_1,t_2,t_3, and t_4) shown in figure 12(b). The overall dimensions b and h are determined from a geometrical procedure[22] which fits a rectangle of maximum area inside the airfoil section. The airfoil section size is determined from the thickness-to-chord ratio (t/c) and the local chord (c). The dimension t_s represents the local thickness of the airfoil (t_s=c*t/c).

Lower Level Design Variables - At each cross section, the lower level design variables are the four wall thicknesses t_1, t_2, t_3, and t_4 as shown in figure 12b for a total of 20 design variables.

Lower Level Constraints - At a given section, the lower level constraints are enforced on the lower level extensional stiffness, cross sectional stresses, and wall thicknesses. The extensional stiffness constraint requires that the lower level EA be greater than the upper level EA^* and is given by

$$1 - EA/EA^* \le 0 \tag{9}$$

where EA is the lower level extensional stiffness and EA^* is the upper level extensional stiffness at the given cross section. It is noted that EA appears in a constraint rather than in the objective function (equation 8) where the other stiffnesses appear. This was done for the following reason. The role of EA in the upper level is limited to satisfying the strain constraint (equation 7). The lower level is responsible only for assuring that the value of EA is at least as large as the value needed in the upper level -- close matching of EA to EA^* is not required.

The stress constraints are evaluated at the corners and midsides of the cross section shown in figure 13.

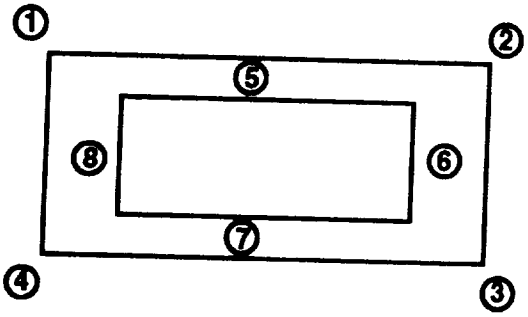

Fig. 13 Locations in cross section for stress calculations

The stress constraints have the following form

$$V(\sigma_x, \sigma_{xy}) / \sigma_a - 1 \le 0 \qquad (10)$$

where $V(\sigma_x, \sigma_{xy})$ is Von Mises stress measure given by

$$V(\sigma_x, \sigma_{xy}) = \sqrt{\sigma_x^2 + 3\sigma_{xy}^2} \qquad (11)$$

where σ_x, σ_{xy} and σ_a are the axial bending stress, shear stress and allowable stress, respectively. The stresses σ_x and σ_{xy} are given by

$$\sigma_x = (M_f / I_f)\xi + (M_l / I_l)\eta + N / A \qquad (12)$$

$$\sigma_{xy} = M_T / (2A_c t) + \frac{SQ}{I_f t} \qquad (13)$$

where M_f is the flapwise moment, M_l is the lag moment, I_f is the flapwise bending inertia, I_l is the lag bending inertia, M_T is the torque at the section; A_c is the area of the cross section enclosed by the centerlines of the walls; t is the side wall thickness; S is the vertical shear force, Q is the usual first moment used in beam shear stress analysis. The terms ξ and η are the principal/centroidal coordinates of the appropriate points in the cross section (figure 13). The moments and the torque,and forces are computed in the upper level and passed to the lower level.

An additional set of constraints is imposed on the lower level design variables to assure that the section remains a thin-walled section. These constraints are as follows

$$t_i / h < 0.1 \qquad i = 2 \text{ and } 4 \qquad (14\,a)$$

$$t_i / h < 0.1 \qquad i = 1 \text{ and } 3 \qquad (14\,b)$$

where b and h are the width and height of the cross section respectively.

Coordination Between Upper and Lower Levels - As mentioned in the section on upper level constraints, the coordination between the upper and lower levels is implemented by upper level constraints. These constraints are imposed to encourage changes in the upper level design variables which promote consistency between the stiffnesses from the upper and lower levels. Specifically, these constraints (one at each of five spanwise stations, figure 12) have the form

$$g = F - (1 + \varepsilon)F_o \le 0 \qquad (15)$$

where F is given by equation (8) for the current upper level design variables, F_O is the latest value of the lower level objective function, and ε is a specified tolerance.

Derivative of Coordination Constraint - The derivative of the constraint in equation (15) is required as part of the optimization (as are the derivatives of all the constraints and the objective functions). The derivative of the coordination constraint involves some complexities which are illustrated herein. In view of equation (8) a constraint g may be written as

$$g = g\{F(X), F_o(X, Q(X))\} \qquad (16)$$

where X is the set of upper level design variables and Q is the set of behavioral quantities which are computed in the upper level and used in the lower level (i.e, M_f, M_l, N). From equation (16)

$$\frac{\partial g}{\partial X} = \frac{\partial g}{\partial F}\frac{\partial F}{\partial X} + \frac{\partial g}{\partial F_o}\frac{\partial F_o}{\partial X} + \frac{\partial g}{\partial F_o}\frac{\partial F_o}{\partial Q}\frac{\partial Q}{\partial X} \qquad (17)$$

where $\frac{\partial g}{\partial F} = 1$, $\frac{\partial F}{\partial X}$ is obtained by differentiating equation (8), $\frac{\partial g}{\partial F_o} = -(1+\varepsilon)$, $\frac{\partial F_o}{\partial X}$ and $\frac{\partial F_o}{\partial Q}$ are derivatives of an optimum design with respect to parameters[23] and $\frac{\partial Q}{\partial X}$ is a behavior sensitivity derivative computed in the upper level.

Overall Organization of ADS Procedure

The overall system is shown schematically in figure 14 and outlined herein. The upper level analysis, as shown in figure 10, is executed for the current set of design variables. This analysis provides all of the information needed to calculate the objective function and constraints with the exception of the coordination constraint (equation 15). The lower level optimization (figure 11) is then performed for each of the five cross sections shown in figure 12 to match (as closely as possible) the current upper level bending and torsional stiffnesses. The lower level optimization also provides the objective function, F_o needed for the coordination constraints. These final constraints, together with the remaining information from the upper level, permit the upper level optimization to take place. This describes one cycle of the procedure. The procedure is repeated for additional cycles until convergence is achieved.

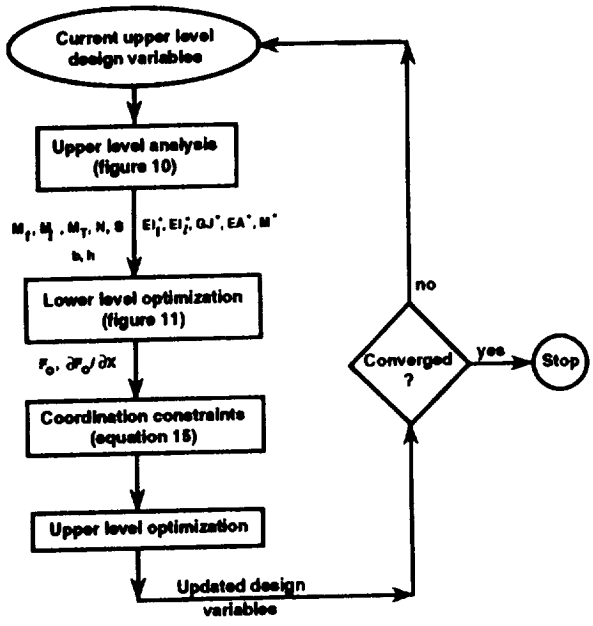

Fig. 14 Overall ADS system implementation

Concluding Remarks

This paper has described a joint activity involving NASA and Army researchers at the NASA Langley Research Center to develop rotorcraft optimization procedures which integrate appropriate disciplines and account for all of the important interactions among the disciplines. The disciplines involved include rotor aerodynamics, rotor dynamics, rotor structures, airframe dynamics, and acoustics. The work is focused on combining the five key disciplines listed above in optimization procedures to satisfy multidisciplinary design requirements. Fundamental to the plan is a three-phased approach. In phase 1, the disciplines of blade dynamics, blade aerodynamics, and blade structure will be closely coupled while acoustics and airframe dynamics will be decoupled and accounted for as effective constraints on the design for the first three disciplines. In phase 2, acoustics is to be integrated with the first three disciplines. Finally, in phase 3, airframe dynamics will be fully integrated with the other four disciplines. The paper described the plan and summarized the most recent results and progress in the work. These include results for optimal placement of tuning mass for reduction of blade vibratory shear forces, results for integrated aerodynamic/dynamic optimization, efforts for validation of the procedures and the formulation of a multilevel integrated aerodynamic/dynamic/structural optimization procedure. The results demonstrate the potential of optimization in design of future rotorcraft, both from the standpoint of efficiency of the process as well as potentially improved products. The results demonstrate that there are significant opportunities awaiting analytical designers who pursue interdisciplinary design approaches. It has been the intention of the authors and the Langley team, in general, to develop the research with the long-term needs of the rotorcraft industry in mind. This paper already reflects a significant industry influence as a result of modifications following industry visits. It is planned to continue this dialogue with the anticipation of additional industry interaction during future phases of this research.

References

1. Ashley, H.: On Making Things the Best-Aeronautical Use of Optimization. Journal of Aircraft, vol. 19, no. 1, 1982.
2. Sobieszczanski-Sobieski, J.: Structural Optimization :Challenges and Opportunities. International Journal of Vehicle Design, Vol. 7, nos. 3-4, 1986.

3. Miura, H.: Application of Numerical Optimization Methods to Helicopter Design Problems: A Survey. NASA TM-86010, October 1984.
4. Bennett, R. L.: Application of Optimization Methods to Rotor Design Problems. Vertica, vol. 7, no. 3, 1982, pp. 201-208.
5. Peters, D. A.; Rossow, M. P.; Korn, A.; and Ko T.: Design of Helicopter Rotor Blades for Optimum Dynamic Characteristics. Computers and Mathematics with Applications, vol. 12A, no. 1, 1986, pp. 85-109.
6. Friedmann, P.: Application of Modern Structural Optimization to Vibration Reduction in Rotorcraft, Vertica, vol. 9, no. 4, 1986, pp. 363-376.
7. Adelman, H. M.; and Mantay, W. R., editors: Integrated Multidisciplinary Optimization of Rotorcraft: A Plan for Development. NASA TM-101617. (Also AVSCOM TM-89-B-004) May 1989.
8. Chattopadhyay, Aditi; and Walsh, Joanne L.: Minimum Weight Design of Rotorcraft Blades with Multiple Frequency and Stress Constraints. NASA TM-100569, March 1988.
9. Pritchard, J. I., and Adelman, H. M., Optimal Placement of Tuning Masses For Vibration Reduction in Helicopter Rotor Blades, NASA TM 100562 AVSCOM TM 88-B-003, March 1988.
10. Pritchard, J. I., Adelman, H. M., Walsh, J. L., Wilbur, M. L., Optimizing Tuning Masses for Helicopter Rotor Blade Vibration Including Computed Airloads and Comparison With Test Data, NASA TM 104194 AVSCOM TM 91-B-020, January, 1992.
11. Davis, M. W.: Optimization of Helicopter Rotor Blade Design for Minimum Vibration. NASA CP-2327, part 2. September 1984, pp. 609-625.
12. Walsh, J. L.; Bingham, G. J.; and Riley, M.F.: Optimization Methods Applied to the Aerodynamic Design of Helicopter Rotor Blades. Journal of American Helicopter Society, October 1987, pp. 39-44.
13. Chattopadhyay, Aditi, Walsh, Joanne L., and Riley, Michael F., Integrated Aerodynamic/Dynamic Optimization of Helicopter Rotor Blades, Journal of Aircraft, vol. 28, no. 1, Jan. 1991.
14. Walsh, Joanne L.; LaMarsh II, William J.; and Adelman, Howard M.: Fully Integrated Aerodynamic/Dynamic Optimization of Helicopter Rotor Blades. NASA TM-104226, February 1992.
15. Nixon M. W.: Preliminary Structural Design of Composite Main Rotor Blades for Minimum Weight. NASA TP-2730, July 1987.
16. Sobieszczanski-Sobieski, J.: A Linear Decomposition Method for Large Optimization Problems--Blueprint for Development. NASA TM-83248, 1982.
17. Sobieszczanski-Sobieski, J.; James, B.; and Dovi, A.: Structural Optimization by Multilevel Decomposition. AIAA Journal, Vol. 23, November 1983.
18. Vanderplaats, G. N.: CONMIN--A Fortran Program for Constrained Function Minimization. User's Manual. NASA TMX-62282, August 1973.
19. Johnson, Wayne: CAMRAD/JA - A Comprehensive Analytical Model of Rotorcraft Aerodynamics and Dynamics - Johnson Aeronautics Version. Volume I:Theory Manual and Volume II: User's Manuals. Johnson Aeronautics, 1988.
20. Gessow, Alfred; and Myers, Garry C., Jr.: Aerodynamics of the Helicopter. Frederick Ungar Publishing Company, New York, 1967.
21. Bruhn,E.F.: Analysis and Design of Flight Vehicle Structures, Jacobs Publishers, Inc. Carmel, Indiana 1973.
22. Walsh, Joanne L.: Computer-aided Design of Light Aircraft to Meet Certain Aerodynamic and Structural Requirements. Master's Thesis. Old Dominion University. August 1973.
23. Sobieszczanski-Sobieski,J., Barthelemy, J.F., and Riley, K. M., Sensitivity of Optimum Solutions to Problem Parameters, AIAA Journal, vol. 20, Sept. 1982, pp. 1291-1299.

REPORT DOCUMENTATION PAGE

Form Approved
OMB No. 0704-0188

1. AGENCY USE ONLY (Leave blank)	2. REPORT DATE	3. REPORT TYPE AND DATES COVERED
	September 1992	Technical Memorandum

4. TITLE AND SUBTITLE

Recent Advances in Multidisciplinary Optimization of Rotorcraft

5. FUNDING NUMBERS

505-63-36-06
1L162211A47A

6. AUTHOR(S)

Howard M. Adelman
Joanne L. Walsh Jocelyn I. Pritchard *

7. PERFORMING ORGANIZATION NAME(S) AND ADDRESS(ES)

NASA Langley Research Center
Hampton, VA 23665-5225
and
Aerostructures Directorate, U.S. Army-AVSCOM
Langley Research Center, Hampton, VA 23665-5225

8. PERFORMING ORGANIZATION REPORT NUMBER

9. SPONSORING/MONITORING AGENCY NAME(S) AND ADDRESS(ES)

National Aeronautics and Space Administration
Washington, DC 20546-0001
and
U. S. Army Aviation Systems Command
St. Louis, MO 63120-1798

10. SPONSORING/MONITORING AGENCY REPORT NUMBER

NASA TM-107665
AVSCOM TR-92-B-012

11. SUPPLEMENTARY NOTES

Presented as an AIAA Paper # 92-4777 at the Fourth AIAA/USAF/NASA/OAI Symposium on Multidisciplinary Analysis and Optimization, September 21-23, 1992, Independence, Ohio.

* U. S. Army-AVSCOM

12a. DISTRIBUTION/AVAILABILITY STATEMENT

Unclassified - Unlimited

Subject Category 05

12b. DISTRIBUTION CODE

13. ABSTRACT (Maximum 200 words)

This paper describes a joint activity involving NASA and Army researchers at the NASA Langley Research Center to develop optimization procedures to improve the rotor blade design process by integrating appropriate disciplines and accounting for all of the important interactions among the disciplines. The disciplines involved include rotor aerodynamics, rotor dynamics, rotor structures, airframe dynamics and acoustics. The work is focused on combining these five key disciplines in an optimization procedure capable of designing a rotor system to satisfy multidisciplinary design requirements. Fundamental to the plan is a three-phased approach. In phase 1, the disciplines of blade dynamics, blade aerodynamics, and blade structure are closely coupled while acoustics and airframe dynamics are decoupled and are accounted for as effective constraints on the design for the first three disciplines. In phase 2, acoustics is integrated with the first three disciplines. Finally, in phase 3, airframe dynamics is integrated with the other four disciplines. Representative results from work performed to date are described. These include optimal placement of tuning masses for reduction of blade vibratory shear forces, integrated aerodynamic/dynamic optimization, and integrated aerodynamic/dynamic/structural optimization. Examples of validating procedures are described.

14. SUBJECT TERMS

blade dynamics, blade aerodynamics, airframe dynamics
optimization multidisciplinary design
integrated aerodynamic/dynamic optimization

15. NUMBER OF PAGES

13

16. PRICE CODE

A03

17. SECURITY CLASSIFICATION OF REPORT	18. SECURITY CLASSIFICATION OF THIS PAGE	19. SECURITY CLASSIFICATION OF ABSTRACT	20. LIMITATION OF ABSTRACT
Unclassified	Unclassified	Unclassified	UL